GEOPHYSICAL RESEARCH LETTERS, VOL. 23, NO. 20, PAGES 2797-2800, OCTOBER 1, 1996

Measurements of superadiabatic lapse rates in the middle atmosphere

R. J. Sica and M. D. Thorsley
Department of Physics and Astronomy, The University of Western Ontario, London, Canada

Abstract. A large power-aperture product Rayleigh-scatter lidar system has been successfully built and over 175 nights of middle atmosphere temperature measurements have been obtained. The high signal-to-noise ratio of these measurements allows the stability of the air in the upper stratosphere and mesosphere to be determined. A detailed methodology has been developed to attempt to differentiate between lapse rate variations due to photon counting errors and actual geophysical variations. On nights when the geophysical variations are large compared to the photon counting errors, regions of convective stability and instability can be determined at a reasonably high confidence level. Both statistics of the layers and an "image" of the layers is presented for the night of May 31, 1996. The measured percentage of unstable layers is in agreement with the predictions of Hines (1991), as is the apparently sporadic formation and distribution of the unstable regions.

Introduction

A problem of both scientific and practical interest in atmospheric science is to quantify the effect of gravity waves generated primarily in the lower atmosphere on the middle and upper atmosphere, both to understand the physics of the wave process, and for improved parameterization schemes for general circulation models. Descriptions of the physics of the wave process based on linear theory have been given to explain the "universal" power law form of the tail spectrum (e.g. *Dewan and Good,* 1986; *Smith et al.,* 1987). These theories assume an instability criterion to generate the tail spectrum. *Hines* (1991) demonstrates how these criteria for single waves can be generalized to a broad spectrum of waves. He also makes predictions for the probability of instability and shows that convective instability is about three times more probable than dynamical instability. Perhaps most importantly, he concludes that a broad spectrum of waves will produce an irregular distribution of small-scale (relative to the low wavenumber end of the tail spectrum) unstable patches, which could influence the formation of the tail spectrum.

Lidar are well suited for extended time series measurements of temperature profiles with sufficient spatial-temporal resolution for determining lapse rate variations. The highest spatial-temporal resolution temperature profiles in the 30 - 80 km region are obtained using Rayleigh-scatter lidar. Rayleigh-scatter lidars have been used to identify large-scale regions where convective instability can occur, such as mesospheric temperature inversions (e.g. *Hauchecorne et al.,* 1987). Temperature measurements in the upper stratosphere from Toronto, Canada have been used to identify large-scale regions of marginal stability, although no evidence for convective instability was found (*Whiteway and Carswell,* 1995). It is significantly more difficult to measure regions of convective instability at the small scales (i.e. < 300 m) relevant to the tail spectrum, since the dry adiabatic lapse rate is only 0.01 K/m. An extremely high signal-to-noise ratio measurement is needed to judge the stability in a narrow height region. The large power-aperture product lidar developed at The University of Western Ontario appears to be capable of identifying regions of stability as well as instability, in the sense that a region of superadiabatic lapse rate is potentially convectively unstable.

Paper number 96GL02642
0094-8534/96/96GL-02642$05.00

The Measurements

The University of Western Ontario's Purple Crow Lidar is a monostatic lidar system which can simultaneously measure both Rayleigh and sodium resonance fluorescence backscatter. The lidar is located just outside of London, Ontario, Canada at the Delaware Observatory (42°52' N; 81°23' W). The Purple Crow Lidar enjoys a large power-aperture product by the use of a high power transmitter and large aperture receiver. The transmitter is a Nd:YAG laser operating at the second harmonic, with a output energy of nominally 600 mJ/pulse at 20 Hz. The receiver is a 2.65-m diameter liquid mercury mirror, which is coupled to a photon counting system by an optical fiber. *Sica et al.* [1995] show that the liquid mirror has a performance similar to a traditional glass telescope of the same area. The large power-aperture product allows high signal-to-noise ratio density fluctuation measurements to be obtained.

The measurements are obtained every 1 min in 24 m range bins. The returned photocounts are converted to density profiles via the lidar equation. Temperatures are found from the density profiles by assuming hydrostatic equilibrium between adjacent atmospheric layers, applying the Ideal Gas Law, integrating the resulting equation and solving for temperature. A particularly clear exposition of this technique is given by *Chanin and Hauchecorne* [1984]. Their formalism is particularly well suited for temperature retrievals, as the density integration is performed over pressure surfaces rather than height surfaces.

Methodology of the Study

The methodology of determining the regions of stability and instability is tedious but needs to be elucidated. In principle one could simply take a temperature profile, differentiate it and be done. In practice, despite the large return photocount signal, the temperature changes sought are extremely small. Furthermore, the expectation is that higher in the atmosphere more unstable regions will exist as the gravity waves' amplitudes increase with height. Unfortunately, the lidar return signal decreases for the same reason, and in fact faster, than the gravity waves grow due to the exponential decrease of density with height. Hence, extreme care must be taken in the determination of stable and unstable regions.

The raw photocount measurements are co-added to 72 m height bins and the individual scans co-added to 15 min in time. The temperature profiles are determined as discussed above. The lapse rates are then calculated using a Parks-McClellan optimal equiripple FIR differentiator (*Oppenheim and Schafer* [1989]). This filter has a bandwidth of 504 m and a passband of 72 m. The filter was extensively tested versus a simple centered derivative method. The advantages of the Parks-McClellan filter is the variance increase of the filter is about half that of a centered derivative, in addition to having a narrower passband. The appropriate dry adiabatic lapse rate is then subtracted from the environmental lapse rate to form a difference. If this difference is less than zero convective instability can occur; if the difference is greater than zero the atmosphere is stable to convection.

The photon noise in the temperature profiles, if sufficiently large, can cause the appearance of superadiabatic regions in an otherwise stable temperature profile. Furthermore, if the unstable regions are isolated in space and time their observational signature will be similar to photon noise. The measurement includes both the atmospheric variance and the photon noise, but since a large number of measurements (about 10,000) are available in an observing period, statistical tests can be used to differentiate between the two variances. To isolate the photon noise contribution to the total variance, a synthetic data set is made using the average density profile from the measurements (to obtain a similar shape for the photocount profile). Each synthetic profile is made at the same heights and times as the measurements and is constructed to have a total photocount equal to the measurements in the clear signal region (45 to 60 km). Gaussian white noise of similar magnitude to the measurements is imposed on each profile. Since on average, the atmosphere is convectively stable, the synthetic profile will have no regions of convective instability which are not due to photon noise. These synthetic data sets will henceforth be called "cloned" data.

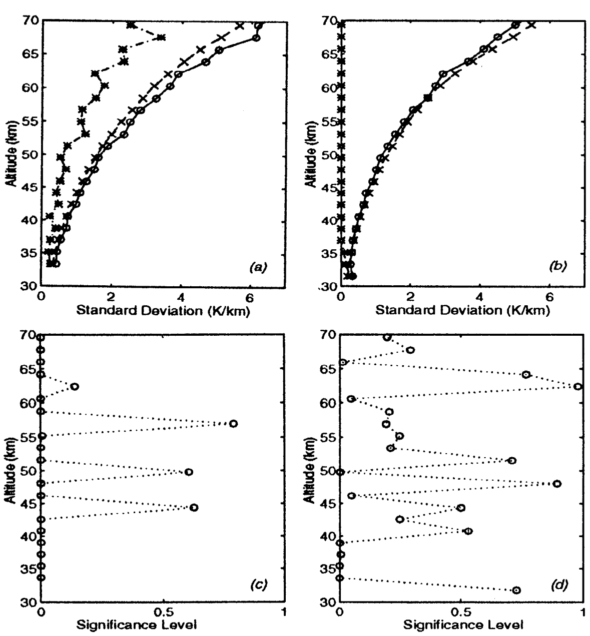

Figure 1. (*a*) The standard deviation of the lapse rate ('o' symbol), the photocount noise ('x' symbol) and the difference between the lapse rate standard deviation and photocount noise ('*') for May 31, 1996. (*b*) Same as (*a*) for October 12, 1994. (*c*) The *F*-test statistic comparing the variance of the lapse rate measurement to the variance due to photon noise for the cloned data on the May night. *F*-test values less than 0.1 suggest a likelihood that the variances are different for the two distributions. (*d*) Same as (*c*) for the October night.

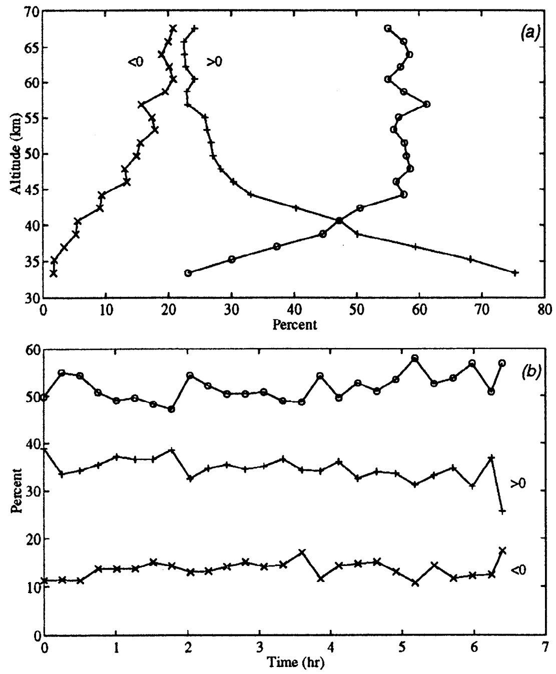

Figure 2. (*a*) The percentage of stable ('+', labelled '> 0'), unstable ('x', labelled '< 0') and indeterminate ('o') regions as a function of altitude over the 6.5 hr observing period on May 31, 1996. (*b*) The percentage of stable ('+', labelled '> 0'), unstable ('x', labelled '< 0') and indeterminate ('o') regions as a function of time over the altitude range shown in (*a*).

Each individual difference between the measured lapse rate and the dry adiabatic lapse rate and cloned data point (and their associated error) is then treated as the mean and variance of a Gaussian distribution. Distributions in which 80% of the probability lies below zero are classified as negative and vice versa for positive. Distributions which fall in neither category are indeterminate. Statistical testing has shown that the assumption of a Gaussian distribution is true a high percentage of the time.

With the differences in lapse rates and their signs available for both the measurements and the cloned data, the two distributions can be tested to determine whether or not they are likely to arise from the same parent population. If their distributions are not the same, the differences are due solely to geophysical variations, since the cloned data set contains only photon noise. Before testing, the measurements are separated into layers 1.8 km in height. This choice of layer width yields about 400 samples over a night's measurements, a sufficient number to insure that the tests are meaningful, but not an overabundance of samples which could detect statistically significant differences which are not physically significant. Kuiper's variant of the Kolmogorov-Smirnov test is used to test whether the measurements and the cloned data are from the same distribution, while the *F*-test is used to test whether the data sets have significantly different variances (*Press et al.* [1992]).

On some nights the results of these tests show height regions where the lapse rate measurements are significantly different from the cloned data. In these regions the measurements can then be used to compute the percentage of space-time the atmosphere is stable or unstable. By counting the size of contiguous stable, indeterminate and unstable regions in space and time histograms of the distribution of layer sizes can be formed (the coherence of the layers). Finally, the measured variance of the lapse rate in each layer can be compared to the photon noise of the measurements, which

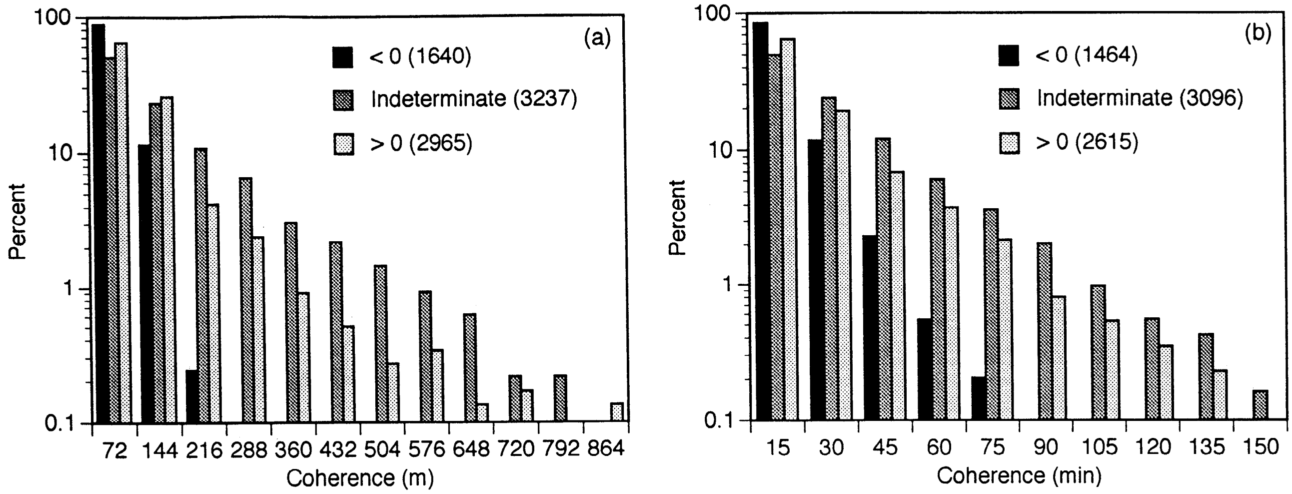

Figure 3. (*a*) Coherence histogram of the number of contiguous stable, unstable and indeterminate regions in the vertical for the 6.5 hr observing period on May 31, 1996. The number of events in each bin is shown in parenthesis. (*b*) Coherence histogram of the number of contiguous stable, unstable and indeterminate regions in time for all heights on May 31, 1996. The number of events in each bin is shown in parenthesis.

provides an independent measure of the difference of the variances.

Results

Twelve nights have initially been examined in detail. Standard deviations and *F*-test results for two nights, May 31, 1996 and October 12, 1994 are shown in Figure 1. Figure 1*a* shows that the May night has larger standard deviation in the lapse rate measurements than the photon noise, as evident in the difference curve. On the October night the lapse rate standard deviation and the photon noise are similar, except at the lowest heights (Figure 1*b*). Note that the photon noise is similar on both nights but the variance of the lapse rate measurements is larger in May. Several other October nights in 1994 also have smaller lapse rate variances, while several other May and June nights in 1996 have larger lapse rate variances.

Both the Kuiper (not shown) and the *F*-tests (Figures 1*c* and 1*d*) are consistent with this interpretation. On the May night the *F*-test values are predominately much less than 0.1, meaning that there is evidence from the measurements that the measurements and cloned data have different variances. With the exception of the lowest altitudes, the October night has Kuiper and *F*-test values consistent with the lapse rate measurements and the cloned data set have similar distributions and variances.

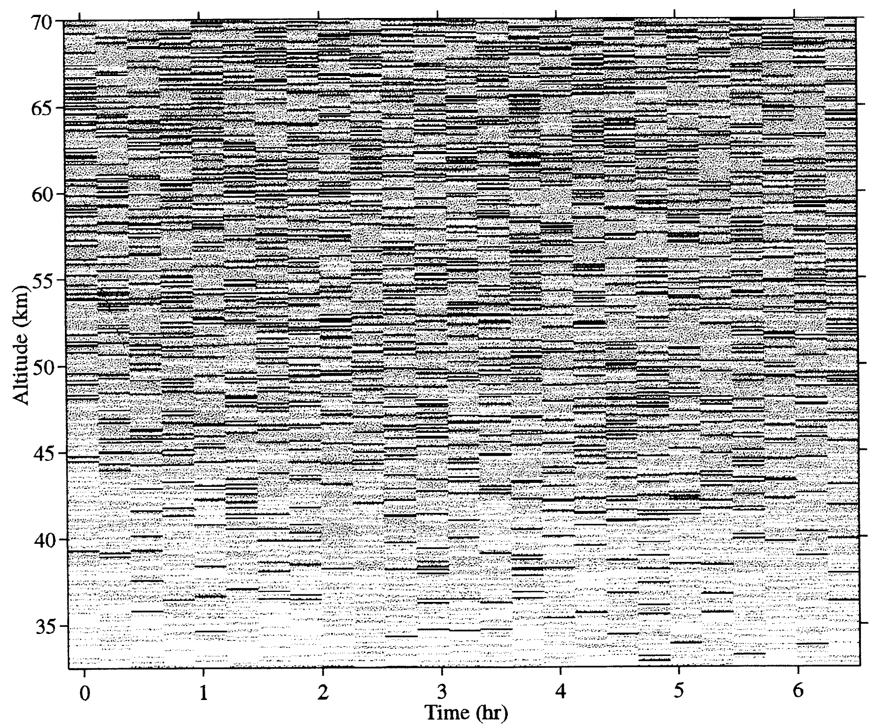

Figure 4. Lapse rate "image" for individual regions on May 31, 1996, coded white for stable, black for unstable and grey for indeterminate. The width of each bin is the duration of the measurement. The probability of a region actually being stable or unstable, given it is marked as such, is 80%. Most of the stable regions occur in the upper stratosphere, while more unstable regions occur in the mesosphere.

Figure 2 shows the height-time percentages for the May night. The percentage of regions with height (Figure 2*a*) shows that above 43 km about 57% of the events are indeterminate. This amount is slightly less than expected from photon noise, as seen in the cloned data set (not shown), and is about 6% less than the October night (not shown). Both the percentage of stable and unstable regions is about 4% greater than the October night (except below 35 km). Moreover, on the October night the height-time percentages were nearly identical for the measurements and cloned data. The percentage of unstable regions increases from 2% at 35 km to 20% near 70 km. More stable regions exist at the lowest heights, decreasing rapidly up to the stratopause. *Hamilton* (1984) computed the Richardson number for a large body of sounding rocket measurements. The nearest station to London, Ontario in his study is Wallops Island, Virginia, about 5^o of latitude to the south. The percentage of regions with $Ri < 1$ for Hamilton's averages during equinox agree well in the stratosphere, but his results are about 40% smaller in the mesosphere. Temporally, there is a slight increase in the percentage of indeterminate regions over the night, with about 53% of the regions indeterminate, 35% stable and 12% unstable (Figure 2*b*).

The coherences are shown in Figure 3. In the vertical, the number of consecutive unstable regions rapidly decreases, with about 90% of the regions less than 144 m in extent (Figure 3*a*). For the stable regions, more than 99% of the measurements have vertical extents less than 360 m. The distribution of the indeterminate regions has an extended tail out to 792 m.

The temporal coherences of the unstable regions also decrease rapidly, though slower than the vertical coherences (Figure 3*b*). Greater than 99% of the unstable regions have durations less than 60 min. Both the stable and indeterminate regions have longer tails. The measurements are presented at the highest spatial-temporal resolution possible that unambiguously shows regions where most of the events are not due to photon noise. It is important bear in mind that over the 15 min time averages unstable regions could form, disappear and reoccur, perhaps several times.

The stability of individual layers is shown as an "image" in Figure 4. The length of each bar corresponds to the 15 min integration, while the width of the bar indicates it's vertical extent. A preponderance of stable regions are evident at all times below 40 km, though unstable regions are also present. Above 40 km the distribution of unstable layers appears sporadic and uncorrelated from scan to scan.

Conclusions

The initial study of a dozen nights of Rayleigh-scatter lidar temperature measurements from the Purple Crow Lidar has shown that, when the variability of the temperature profiles is large enough on an individual night, regions of stable and unstable air can be identified with a reasonably high degree of confidence. On nights such as May 31, 1996 the measured lapse rate differences are statistically different from the lapse rate differences due solely to instrumental noise.

The percentage of known stable regions on the May night decreases rapidly in the upper stratosphere to the stratopause, from 75% to 25%. The percentage of known unstable regions increases roughly monotonically from a few percent at 35 km to about 20% at 70 km. The percentage of known unstable regions is consistent with the calculations of *Hines* (1991) for the probability of unstable convective layers resulting from a broad spectrum of waves. The temporal and spatial coherence of the known unstable regions decreases rapidly with bin size: 99% of the known unstable regions have coherences less than 216 m in vertical extent and temporal scales less than 60 min.

The measurements appear to support the interpretation of *Hines* (1991) that these unstable regions are the "whitecaps" of gravity waves who's phase velocities are such that they are about to be removed from the spectrum. The generation of these regions, particularly in the mesosphere, appear to be random in the sense the regions seem to form sporadically and to be relatively localized in space and time. Further studies using the available measurements from the Purple Crow Lidar are now in progress to address the day-to-day and seasonal variability of the layers.

Acknowledgments. We would like to thank Drs. S. Argall, C. Gardner, K. Hamilton, C. Hines, J. MacKay, M. McIntyre and T. Shepherd for inspiring discussions and suggestions on this study, Mr. S. D. Beatty for visualization engineering and the referees for their helpful comments. This work was made possible by grants from the National Science and Engineering Research Council, the Canadian Space Agency and the Atmospheric Environment Service.

References

Chanin, M. L.and A. Hauchecorne, Lidar studies of temperature and density using Rayleigh scattering, in *Handbook for MAP: Ground-Based Techniques,* **13**, ICSU Scientific Committee on Solar Terrestrial Physics, Urbana, Illinois, paper 7, 1984.

Dewan, E. M. and R. E. Good, Saturation and the "universal" spectrum for vertical profiles of horizontal scalar winds in the atmosphere, *J. Geophys. Res.*, **91**, 2742-2748, 1986.

Hamilton, K., A study of the occurrence of dynamically unstable conditions in the middle atmosphere, *Can. J. Phys.*, **62**, 963-967, 1984.

Hauchecorne, A., M. L. Chanin, and R. Wilson, Mesospheric temperature inversion and gravity wave breaking, *Geophys. Res. Lett.*, **14**, 933-936, 1987.

Hines, C. O., The saturation of gravity waves in the middle atmosphere. Part I: Critique of linear-instability theory. *J. Atmos. Sci.*, **48**, 1348-1359, 1991.

Oppenheim, A. V. and R. W. Schafer, *Discrete-Time Signal Processing*. Prentice-Hall, Inc., 256-266, 1989.

Press, W. H., S. A Teukolsky, W. T. Vetterling, and B. P. Flannery., *Numerical Recipes in FORTRAN, the Art of Scientific Computing*, 2nd edition. Cambridge University Press, 613-622, 1992.

Sica, R. J., S. Sargoytchev, P. S. Argall, E. F. Borra, L. Girard, C. T. Sparrow, and S. Flatt, Lidar measurements taken with a large-aperture liquid mirror. 1. Rayleigh-scatter system. *Appl. Opt.*, **34**, 6925-6936, 1995.

Smith, S. A., D. C. Fritts, and T. E. Van Zandt, Evidence for a saturated spectrum of atmospheric gravity waves. *J. Atmos. Sci.*, **44**, 1404-1410, 1987.

Whiteway, J. A. and A. I. Carswell, Lidar observations of gravity wave activity in the upper stratosphere over Toronto, *J. Geophys. Res.*, **100**, 14113-14124, 1995.

R. J. Sica and M. D. Thorsley, Department of Physics and Astronomy, The University of Western Ontario, London, Ontario, Canada N6A 3K7. (e-mail: sica@uwo.ca)

(Received June 24, 1996; revised: July 12, 1996; accepted August 21, 1996.)